Microscopic description of α decay from superdeformed nuclei

D. S. Delion

Institute of Physics and Nuclear Engineering, Bucharest Măgurele, POB MG-6, Romania

R. J. Liotta

KTH, Physics at Frescati, Frescativägen 24, S-10405 Stockholm, Sweden

A microscopic formalism to treat α decay from superdeformed nuclei is given within the framework of the Hartree-Fock-Bogoliubov approximation. The process of penetration through the deformed barrier is described exactly. The influence of the deformation on the formation amplitude and on the penetrability is analyzed. It is found that the results of the WKB approximation differ strongly from the exact ones as the deformation increases for β_2 larger than 0.3. The most favorable case that we found corresponds to a superdeformed band in ^{192}Pb, for which the α decay probability is very large, making this a likely mechanism to feed the daughter nucleus ^{188}Hg. [S0556-2813(98)02010-X]

I. INTRODUCTION

Superdeformed nuclei have been intensively investigated, both experimentally [1] and theoretically [2], during the last decade. One of the important questions raised by these studies is the possibility of an α decay branch connecting members of superdeformed bands in the mother nucleus with the ground band in the daughter nucleus. To make a theoretical estimation of those transitions one has to determine whether the formalisms usually applied to study α decay from deformed nuclei are also valid for the case of superdeformations. In particular, the validity of the widely used WKB approximation in computing the penetration of the Coulomb barrier may be questioned. Perhaps even more important, one has to have a reliable method to evaluate the α particle formation amplitude on the surface of the rapidly rotating nucleus in order to evaluate the absolute α decay width. That is, an estimation of the probability of observing α (or even cluster) decay from superderformed nuclei requires a comparison of α decay with other competing modes. This can be done by using the same techniques as in the analysis of the structure of superdeformed bands, i.e., by means of a cranked Hartree-Fock-Bogoliubov (HFB) approximation [3]. Within this approach one would be able to describe, e.g., the expected influence of large quadrupole deformations and pairing correlations on the rotational motion and, therefore, on the α particle formation process. It is expected that a very large single-particle (SP) basis is needed to realize that microscopic treatment. One knows that already the description of spectroscopic properties such as energy levels, electromagnetic transitions or moments of inertia requires the use of rather large SP basis (up to 6–8 major shells) in the diagonalization of the deformed Woods-Saxon potential [4–7]. But in α decay the situation is even more demanding since one has to describe the motion of the four nucleons that eventually become the α particle well outside the surface of the nucleus, where the nuclear interaction between the α cluster and the daughter nucleus (as well as the corresponding effects induced by the Pauli principle) are negligible. One therefore needs very high lying SP orbits in the basis,

i.e., orbits with wave functions extending far out in space [8–10]. In order to avoid the use of very large bases (with all the problems connected with the handling of such bases) we have recently proposed an efficient technique to account for configurations lying high up in the nuclear continuum [11–13].

The aim of this paper is to present a formalism that overcomes the two problems mentioned above, that is one that would allow one to evaluate the penetrability exactly and which would be able to describe the clusterization of the α particle at large distances. We will first solve exactly the quantum mechanics problem of penetration of a particle through a deformed barrier. We will also analyze some selected examples to probe the range of validity of traditional approaches to this problem (e.g., WKB) for the case of superderformed nuclei. A convenient SP basis for our purposes will be presented. This basis will be used to estimate microscopic α particle formation amplitudes in rapidly rotating superdeformed nuclei. In Sec. II we present the formalism, in Sec. III are the applications, and a summary and conclusions are in Sec. IV.

II. FORMALISM

A. α particle dynamics

In this section we will derive a formalism to evaluate exactly the quantum-mechanical penetration of a particle through a deformed barrier. The decay process to be considered is, in standard notation, $B(I_iK_i) \rightarrow A(I_fK_f) + \alpha(l)$. The total decay width corresponding to this process can be estimated by [14]

$$\Gamma \equiv \sum_l \Gamma_l = \lim_{R \to \infty} \hbar v \sum_l |C^{I_i lI_f}_{K_i K_f - K_i K_f} g_l(R)|^2, \quad (2.1)$$

where C is a Clebsh-Gordan coefficient, v is the velocity of the α particle, and $g_l(R)$ is the l component of the wave function describing the relative motion of the α particle with respect to the daughter nucleus. This function can be evaluated by solving the coupled system of equations describing

the motion of the α particle in the deformed potential. Thus, assuming that $V_{ll'}(r)$ is the matrix element connecting the channels l and l' one gets

$$\left\{ -\frac{\hbar^2}{2M_\alpha}\frac{d^2}{dr^2} + \frac{\hbar^2 l(l+1)}{2M_\alpha r^2} \right\} g_l(r) + \sum_{l'} V_{ll'}(r)g_{l'}(r)$$
$$= E_\alpha g_l(r). \qquad (2.2)$$

Due to the Coulomb barrier, which can be very large, the wave function decreases by many orders of magnitude from the nuclear surface to the outer turning point. This makes impossible a forward integration procedure starting from known values on the nuclear surface, since the exponentially increasing solution makes the process unstable. The system of equations (2.2) can be numerically integrated starting from large distances into a stable backward direction, using, for instance, the Numerov iterative procedure [15]. An important test of the accuracy of the calculation is to reproduce the irregular Coulomb waves $G_l(R)$ for a spherical barrier. We have thus calculated the outgoing wave function corresponding to the nucleus $A = 152, Z = 66$ which, after an increase of 12 orders of magnitude inside the barrier, is calculated on the nuclear surface with a precision of 5 digits. Even for a very deformed nuclear surface ($\beta = 0.6$) the interaction matrix $V_{ll'}$ has fast decreasing nondiagonal elements with respect to the difference $|l - l'|$. In principle $l = 10$ partial waves could describe the wave function with a good accuracy. Indeed, by increasing this basis up to $l = 30$ the corrections are negligible. Anyway taking into account that we need high angular momenta to describe an α decay process with a large momentum transfer we considered in our calculation $l = 30$ partial waves.

In order to integrate the system (2.2) starting from large distances, but with a matching condition on the nuclear surface, let us introduce the matrix of the fundamental system of solutions, defined in such a way that at large distances R (where the interaction can be considered spherically symmetric and only the Coulomb interaction is important) it becomes practically a diagonal matrix of the spherical outgoing Coulomb waves, i.e.,

$$S_l^{(k)}(R) \rightarrow \delta_{kl}[G_l(R) + iF_l(R)]. \qquad (2.3)$$

In practice the distance R is usually determined by the outer turning point. A general solution to Eq. (2.2) is built as a superposition of the fundamental solutions. One gets,

$$g_l(R) = \sum_k S_l^{(k)}(R)C_k \rightarrow C_l[G_l(R) + iF_l(R)]. \qquad (2.4)$$

Since the regular Coulomb functions $F_l(R)$ have vanishing values inside the barrier the constants C_k are practically real numbers. These numbers are determined by matching the outgoing solution $g_l(R)/R$ of the Schrödinger equation with the corresponding internal solution. This is the formation amplitude $\mathcal{F}_l(\vec{R}_\alpha)$ defined by [16]

$$\mathcal{F}_l(\vec{R}_\alpha) = \int [\Psi_\alpha(\xi_\alpha)\Psi_A(\xi_A)Y_l(\hat{R})]_{I_i}^* \Psi_B(\xi_B)d\xi_\alpha d\xi_A, \qquad (2.5)$$

where the notation is standard, in particular ξ are internal coordinates. One thus obtains

$$\frac{g_l(R_\alpha)}{R_\alpha} \equiv \frac{1}{R_\alpha}\sum_k S_l^{(k)}(R_\alpha)C_k = \mathcal{F}_l(R_\alpha). \qquad (2.6)$$

Let us stress once more that R_α is a point beyond the nuclear surface, where the cluster is already formed. At this point only the Coulomb interaction is important and the α decay problem can be considered as a two-body problem. The exact expression for the α decay width, Eq. (2.1), becomes

$$\Gamma = \hbar v \sum_l \left[C_{K_iK_f - K_iK_f}^{I_ilI_f} \frac{1}{G_l(R_\alpha)} \sum_{l'} K_{ll'}R_\alpha \mathcal{F}_{l'}(R_\alpha) \right]^2, \qquad (2.7)$$

which has a similar analytic form as the corresponding WKB expression of Ref. [14]. However the matrix K of that reference is here the inverse matrix of the fundamental system of solutions at the matching radius. That is, from Eq. (2.4) and since F_l is negligible one obtains

$$K_{ll'} = G_l(R_\alpha)[S^{-1}(R_\alpha)]_{l'}^{(l)}. \qquad (2.8)$$

Recently an approximate form of this matrix was proposed in Ref. [17].

B. α particle formation amplitude

The other important element in the α decay process is the formation amplitude which, as described above, enters as a boundary condition in Eq. (2.7). To evaluate the formation amplitude we will describe the internal wave functions of the mother and daughter nuclei using a cranked HFB approach for neutrons and protons. We will not include explicitly the neutron-proton interaction although, as usual, that interaction will be taken into account effectively since the strength of the interactions will be adjusted to reproduce the neutron and proton gaps [16].

The dynamics of the rotating system of protons ($\tau = \pi$) and neutrons ($\tau = \nu$) in the daughter nucleus is therefore determined by the following constrained Hamiltonian:

$$H_{A\tau}^{(\omega)} = \sum_{kl} \epsilon_{A\tau;kl}a_{\tau k}^+a_{\tau l} - G_{A\tau}\sum_{kl>0} a_{\tau k}^+ a_{\tau \bar{k}}^+ a_{\tau \bar{l}}a_{\tau l},$$

$$\epsilon_{A\tau;kl} = (E_{A\tau m} - \lambda_{A\tau})\delta_{kl} - \hbar\omega_A(j_x)_{A;kl}, \qquad (2.9)$$

where the index k labels the available quantum numbers, which in this case are the energy E and the projection m of the angular momentum. The operator $a_{\tau k}^+$ creates the daughter SP state $|\psi_{A\tau k}\rangle$, $E_{A\tau m}$ is the energy of the deformed daughter nucleus and $\lambda_{A\tau}$ the Lagrange multiplier that takes into account the conservation in average of the number of particles. In the same fashion, the last term takes into account the conservation in average of the angular momentum along the x axis, with the angular frequency ω as a Lagrange multiplier, i.e.,

$$\sum_{\tau kl} (j_x)_{A\tau;kl}\rho_{A\tau;kl} = \sqrt{I_A(I_A+1)}, \quad \rho_{A\tau;kl} = \sum_i V_{A\tau;li}V_{A\tau;ki}^*, \qquad (2.10)$$

where $V_{A\tau;ki}$ are the HFB amplitudes defined by Eq. (2.11). A similar Hamiltonian is taken for the mother nucleus.

The HFB transformation can be written in a general form as (where we dropped all indices)

$$\begin{pmatrix} \alpha^+ \\ \alpha \end{pmatrix} = \begin{pmatrix} U_A^T & V_A^T \\ V_A^+ & U_A^+ \end{pmatrix} \begin{pmatrix} a^+ \\ a \end{pmatrix}, \quad \begin{pmatrix} \beta^+ \\ \beta \end{pmatrix} = \begin{pmatrix} U_B^T & V_B^T \\ V_B^+ & U_B^+ \end{pmatrix} \begin{pmatrix} b^+ \\ b \end{pmatrix},$$
(2.11)

where a^+ (b^+) creates a normal particle and α^+ (β^+) creates a quasiparticle in the daughter (mother) nucleus. The HFB amplitudes defined above are found by the standard procedure described, for instance, in Ref. [3].

We assume that the two nuclei have different deformations. Yet, their wave functions are connected by the Hermitian transformation

$$\begin{pmatrix} b^+ \\ b \end{pmatrix} = \begin{pmatrix} D^* & 0 \\ 0 & D \end{pmatrix} \begin{pmatrix} a^+ \\ a \end{pmatrix},$$

$$D_{kk'}^* = \langle 0 | a_k b_{k'}^+ | 0 \rangle \equiv \langle \psi_{Ak} | \psi_{Bk'} \rangle. \qquad (2.12)$$

From this equation and Eq. (2.11) one can readily obtain a relation between the vectors (β^+, β) and (α^+, α).

The two HFB vacua $|\Psi_X\rangle$, $X = A, B$ are connected according to the Thouless theorem, i.e. [18],

$$|\Psi_B\rangle = \langle \Psi_A | \Psi_B \rangle \exp\left(\sum_{k<k'} Z_{kk'} \alpha_k^+ \alpha_{k'}^+ \right) |\Psi_A\rangle,$$

$$Z = (VU^{-1})^* = -Z^T. \qquad (2.13)$$

In order to compute the formation amplitude defined by Eq. (2.5) we expand the mother wave function in terms of the tensorial product of the daughter wave function times the two-neutron and two-proton wave functions

$$\Psi_{A+2} = \sum_{k>0} B(k) \mathcal{A}[\psi_{A;k}(1)\psi_{A;\bar{k}}(2)\Psi_A]. \qquad (2.14)$$

If one neglects the antisymmetrization between the core and the cluster [19] the coefficient $B(k)$ is given by the pairing density

$$B(k) = \langle \Psi_{A+2} | a_k^+ a_{\bar{k}}^+ | \Psi_A \rangle$$

$$= \langle \Psi_{A+2} | \Psi_A \rangle (V_A U_A^+ + U_A^* Z^* U_A^+)_{k\bar{k}}. \qquad (2.15)$$

Using standard recoupling technique one gets the formation amplitude in terms of the pairing proton and neutron densities given by Eq. (2.15). The multipole expansion of the formation amplitude is given in Eq. (A2). This is an exact expression, depending upon the relative and center of mass (c.m.) quantum numbers corresponding to the proton and neutron pairs. It is worthwhile to point out that due to the nonorthogonality of the SP basis used in the calculation, as described in the next paragraph, it was necessary to use generalized Talmi-Moshinsky brackets with different harmonic oscillator (HO) parameters [20]. It is also important to mention that this expansion converges rather fast as a function of the radial quantum numbers n_π, n_ν, which define the overlap

integrals. In our calculation it was sufficient to consider $n_\pi, n_\nu \lesssim 8$ to get a good accuracy. The results are stable with respect to increases of these quantum numbers.

C. Single particle basis

In order to ensure a proper asymptotic behavior of the SP wave functions entering Eq. (2.14) we generalize the expansion presented in Ref. [12] to an axially deformed mean field. In that reference the SP representation was chosen to be the eigenstates of two HO potentials. The low lying shells of the representation are eigenvalues of a standard HO, i.e., one that reproduces the bound properties of the nucleus, while the high lying members are eigenvalues of a shallow potential, with eigenfunctions that extend far out in space. The deformed SP states can then be written as

$$\psi_{X\tau;Em}(\xi) = \sum_{2n_1+l_1=N_1 \leqslant N_0} c_{X\tau;E\gamma_1 m}^{(1)} \psi_{\gamma_1 m}^{(\lambda_1)}(\xi)$$

$$+ \sum_{2n_2+l_2=N_2 > N_0} c_{X\tau;E\gamma_2 m}^{(2)} \psi_{\gamma_2 m}^{(\lambda_2)}(\xi),$$
(2.16)

where $X = A, B$, $\gamma = (nlj)$, and

$$\psi_{nljm}^{(\lambda)}(\xi) = [\Phi_{nl}^{(\lambda)}(\vec{r})\chi_{1/2}(s)]_{jm}$$

$$\equiv R_{nl}^{(\lambda)}(r)[i^l Y_l(\hat{R})\chi_{1/2}(s)]_{jm}. \qquad (2.17)$$

Here λ_1 is the HO parameter corresponding to the HO potential which provides the discrete spectrum, while λ_2 describes the quasicontinuum part of the spectrum. The standard representation generally used [6] to diagonalize the mean field includes only the terms corresponding to the first summation in Eq. (2.16) with a given number N_0 of major shells. As shown in Ref. [12], if λ_2 is small (corresponding to the flat HO potential, with wave functions extending far out in space) the description of the mother wave function at large distances is improved.

This basis is able to simultaneously describe the absolute decay width and the spectroscopic factor with the relatively small dimension of 10–11 major shells. It has the saturation property that its further increase does not significantly change the results.

By considering the equations for the HO radial wave function of the parameter λ

$$-\frac{\hbar\omega}{2\lambda}\left[\frac{1}{r}\frac{d^2}{r^2}r - \frac{l(l+1)}{r^2}\right]R_{nl}^{(\lambda)}(r)$$

$$\equiv H_l^{(\lambda)}R_{nl}^{(\lambda)}(r) = \hbar\omega\left(2n+l+\frac{3}{2}-\frac{\lambda r^2}{2}\right)R_{nl}^{(\lambda)}(r),$$
(2.18)

one obtains the following system of algebraic equations in a block-matrix form, for a given projection m:

$$\begin{pmatrix} \mathcal{H}^{(11)}_{\gamma_1\gamma'_1m} & \mathcal{H}^{(12)}_{\gamma_1\gamma'_2m} \\ \mathcal{H}^{(21)}_{\gamma_2\gamma'_1m} & \mathcal{H}^{(22)}_{\gamma_2\gamma'_2m} \end{pmatrix} \begin{pmatrix} c^{(1)}_{X\tau;E\gamma'_1m} \\ c^{(2)}_{X\tau;E\gamma'_2m} \end{pmatrix}$$

$$= E_m \begin{pmatrix} \mathcal{I}^{(11)}_{\gamma_1\gamma'_1} & \mathcal{I}^{(12)}_{\gamma_1\gamma'_2} \\ \mathcal{I}^{(21)}_{\gamma_2\gamma'_1} & \mathcal{I}^{(22)}_{\gamma_2\gamma'_2} \end{pmatrix} \begin{pmatrix} c^{(1)}_{X\tau;E\gamma'_1m} \\ c^{(2)}_{X\tau;E\gamma'_2m} \end{pmatrix}, \quad (2.19)$$

where the summation over γ'_k is understood. The overlap integrals are defined as

$$\mathcal{I}^{(ik)}_{\gamma_i\gamma'_k} = \langle R^{(\lambda_i)}_{n_i l} | R^{(\lambda_k)}_{n'_k l} \rangle \delta_{ll'} \delta_{jj'}, \quad (2.20)$$

while the Hamiltonian kernels are given by

$$\mathcal{H}^{(ik)}_{\gamma_i\gamma'_k m} = \hbar\omega f_k \left[\left(2n'_k + l + \frac{3}{2} \right) \mathcal{I}^{(ik)}_{\gamma_i\gamma'_k} - \frac{1}{2}\langle R^{(\lambda_i)}_{n_i l} | \lambda_k r^2 | R^{(\lambda_k)}_{n'_k l} \rangle \right]$$

$$\times \delta_{ll'}\delta_{jj'} + \langle \psi^{(\lambda_i)}_{n_i ljm} | V | \psi^{(\lambda_k)}_{n'_k l'j'm} \rangle, \quad (2.21)$$

where

$$f_k = \frac{\lambda_k}{\lambda_0}, \quad k=1,2. \quad (2.22)$$

If one considers only even multipolarities the system (2.19) splits into blocks with the same parity. The procedure to diagonalize this system of equations is described in Ref. [12]: one builds a new orthonormal SP basis using the eigenstates of the metric matrix (2.20).

III. APPLICATIONS

We will first test our method in a known case and then we will apply it to a superdeformed nucleus. We thus first analyze the decay $^{152}\text{Dy} \rightarrow {}^{148}\text{Gd} + \alpha$ for which the ground state to ground state (g.s. to g.s.) α decay half live is 8.6×10^6 s [21] and $Q_\alpha = 3.37$ MeV. To simplify the analysis we have chosen the same deformation for the mother and daughter nuclei, i.e., $\beta = 0.2$. This value is realistic in these nuclei. The pairing gaps were adjusted using the masses of neighboring nuclei. We have chosen the universal parametrization of the Wood-Saxon potential given in Refs. [5–7]. The two potentials that define our representation in Eq. (2.16) have different HO parameters. The first $N_1 = 0-6$ major shells of the representation correspond to the eigenvalues of a HO potential with the standard parameter $\lambda_1 = 1.2M_0\omega/\hbar$ [6], while for the higher lying shells, i.e., the shells $N_2 = 7 - 10$, we use $\lambda_2 = 0.7M_0\omega/\hbar$ [12]. This parametrization is fixed by physical constraints. If for instance one takes $N_1 = 0-5, N_2 = 6-9$ one can reproduce the total width, but the spectroscopic factor is overestimated by one order of magnitude and the moment of inertia by a factor of 2. It is worthwhile to stress that the members of the SP representation lying close to the Fermi surface determines the HFB calculation while high lying configurations ensure a proper description of the radial wave functions at large distances. We reproduced the total width, as can be seen in Table I, using the quadrupole deformation $\beta = 0.2$.

TABLE I. Ratio between the theoretical and experimental α decay widths corresponding to the transition $^{152}\text{Dy} \rightarrow {}^{148}\text{Gd} + \alpha$ as a function of the quadrupole deformation parameter. The Q value corresponds to the g.s. to g.s. transition. The width Γ_{WKB} was calculated according to the formalism of Ref. [14] while Γ_{cc} is the one calculated within the formalism presented in this paper.

β	$\Gamma_{\text{WKB}}/\Gamma_{\text{exp}}$	$\Gamma_{cc}/\Gamma_{\text{exp}}$
0.0	0.65	0.65
0.1	0.73	0.69
0.2	1.02	0.75
0.3	1.86	0.98
0.4	4.01	1.52
0.5	9.32	2.46
0.6	27.87	3.48
0.7	101.50	4.97
0.8	450.80	6.90

As usual, we have probed the reliability of our calculation by checking that the total width is approximately independent upon the distance in the region of the touching point, i.e., at $R_\alpha = 8 - 10$ fm. All our calculations are performed in this interval. Moreover, another feature which is worthwhile to stress is that we reproduced the experimental width by using realistic deformations (as given by electromagnetic transitions) and experimental gap values. This is important concerning the reliability of the results in the new region of superdeformations that we will explore below.

Large deformations may invalidate approximate treatments of the penetration problem, particularly the classical WKF approach of Ref. [14]. We give in Table I the ratios theoretical/experimental values of the widths for two cases. In the second column the penetration was calculated by following the WKB approach mentioned above, while in the last column we used the exact coupled channel approach developed in this paper. One can clearly observe that for values of the deformation parameter larger than $\beta = 0.2$ the differences between the ratios in those two columns increase with the deformation. The WKB approximation overestimates strongly the value of the width for large deformation. This is a very important result, since it invalidates calculations of the widths in superdeformed nuclei performed within the WKB.

For the superdeformed band of the mother nucleus ^{152}Dy we have chosen a deformation $\beta_B = 0.6$ for all angular momenta, which is close to the predicted value of Ref. [22]. In order to study the effect of the deformation we have also chosen for it an intermediate value $\beta_B = 0.4$ which corresponds to a superdeformed band in ^{192}Pb [23]. The half life of the g.s. to g.s. decay $^{192}\text{Pb} \rightarrow {}^{188}\text{Hg} + \alpha$ is close to the previous case, i.e., it is 4.0×10^6 s [21], but with $Q_\alpha = 5.22$ MeV, which is larger than before. For the daughter nucleus in the ground state we keep the deformation $\beta_A = 0.2$ used above. The angular momenta are $\omega_A = I_A = 0$.

In the second column of Table II is given the ratio between the pairing gap at a given frequency ω and the one at $\omega = 0$. As perhaps expected, one sees that the gap decreases with the frequency. This behavior is consistent with constant proton and neutron pairing strengths. The angular momenta of the mother nucleus computed according to Eq. (2.10) with

TABLE II. Ratio between the pairing gap Δ at frequency $\hbar\omega$ (given in MeV in the first column) and the corresponding gap at frequency $\hbar\omega=0$ (second column). Angular momentum of the mother nucleus ^{152}Dy corresponding to the quadrupole deformation $\beta_B=0.6$ (third column, labeled I_1) and of the mother nucleus ^{192}Pb with $\beta_B=0.4$ (fourth column, labeled I_2). The product of the proton and neutron overlap integrals entering Eq. (2.15) are given in the fifth column for ^{152}Dy (i.e., $\mathcal{I}_1$, corresponding to $\beta_B=0.6$) and in the last column for ^{192}Pb (i.e., $\mathcal{I}_2$, corresponding to $\beta_B=0.4$). In these two last columns the quadrupole deformations of the daughter nuclei were chosen to be the same, i.e., $\beta_A=0.2$.

$\hbar\omega$	Δ/Δ_0	I_1	I_2	$\mathcal{I}_1$	$\mathcal{I}_2$
0.0	1.00	0	0	1.05($-$2)	3.22($-$1)
0.1	0.98	2	2	1.02($-$2)	3.19($-$1)
0.2	0.92	6	4	2.85($-$2)	3.10($-$1)
0.3	0.82	12	8	6.80($-$3)	2.86($-$1)
0.4	0.68	22	20	2.44($-$3)	9.23($-$2)
0.5	0.50	28	30	8.10($-$4)	3.45($-$2)
0.6	0.35	36	38	2.65($-$4)	5.09($-$4)
0.7	0.25	42	42	8.45($-$5)	1.08($-$4)
0.8	0.19	50	46	2.38($-$5)	1.05($-$5)
0.9	0.15	54	52	8.21($-$6)	3.24($-$6)
1.0	0.12	62	58	1.87($-$6)	4.00($-$6)

quadrupole deformation $\beta_B=0.6$, are given in the third column of that table under the head I_1, while in the fourth column, under the head I_2, are given the angular momenta for $\beta_B=0.4$. The corresponding values for the proton times neutron overlap integrals entering Eq. (2.15) are given in the last two columns. One can see that the overlap decreases by increasing the difference between the mother and daughter deformation parameters.

Our interest is to compare α decay transitions from superdeformed bands with the corresponding g.s. to g.s. transition. This comparison can conveniently be performed by studying the ratio between those two decay widths. Moreover, one can examine separately the nuclear structure part and the penetration part in a convenient fashion by taking the logarithm of the ratio between a partial l component of the total width in Eq. (2.1) and the corresponding experimental value, i.e.,

$$\ln\frac{\Gamma_l}{\Gamma_{\exp}}=\ln\left[C_{K_iK_f-K_iK_f}^{I_i l I_f}\sum_{l'}K_{ll'}R_\alpha\mathcal{F}_{l'}(R_\alpha)\right]^2$$

$$+\ln\frac{\hbar v}{G_l^2(R_\alpha)\Gamma_{\exp}}\equiv\gamma_l^{(1)}(\beta_A,\beta_B,\omega)+\gamma_l^{(2)}(Q_\alpha).$$

$$(3.1)$$

The behavior of the formation amplitude, contained in the quantity $\gamma_l^{(1)}$, is shown in Fig. 1 as a function of the rotational frequency.

In Fig. 1(a) we present the function $\gamma_l^{(1)}$ corresponding to the decay from the superdeformed band in ^{152}Dy. The deformation parameters are $\beta_A=0.2$ and $\beta_B=0.6$. The curves are labeled by the angular momentum of the α particle l. In Fig. 1(b) we present the same quantity corresponding to the decay of ^{192}Pb, for which it is $\beta_A=0.2$, $\beta_B=0.4$.
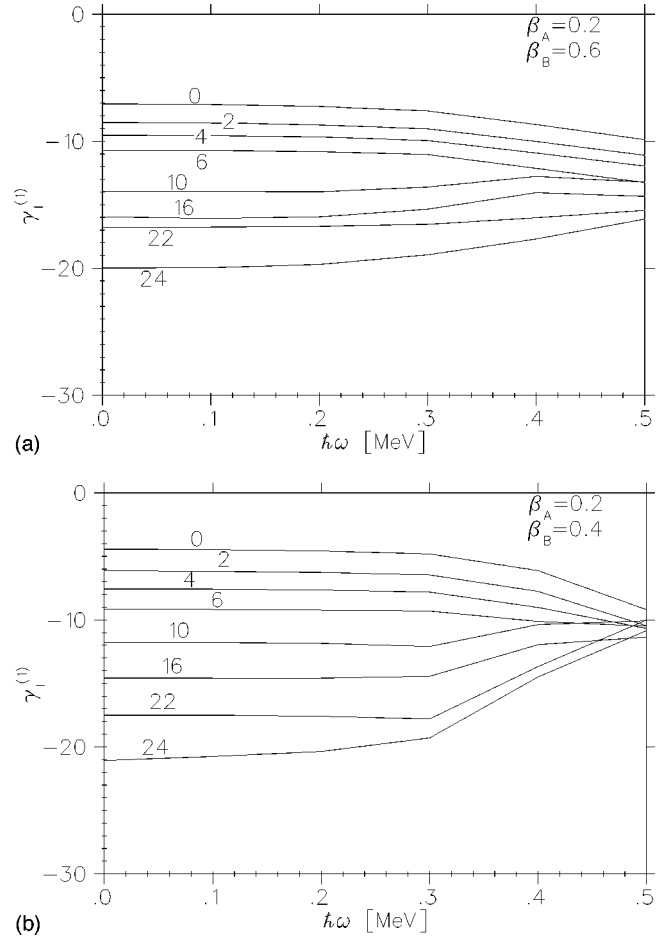

FIG. 1. (a) The number $\gamma_l^{(1)}$ containing the formation amplitude [see Eq. (3.1)] as a function of the rotational frequency $\hbar\omega$ (in MeV) for the α decay from ^{152}Dy. The deformation parameters for the mother and daughter nuclei are $\beta_A=0.2$, $\beta_B=0.6$. (b) As in (a) for the decay of ^{192}Pb, corresponding to $\beta_A=0.2$ and $\beta_B=0.4$. The curves are labeled by the corresponding l values.

One notices in these figures a rather abrupt change in the formation amplitude for $\hbar\omega$ at about 0.3 MeV. This is due to a corresponding change in the pairing density distribution, which sharply decreases around the Fermi level with the rotational frequency in that range of $\hbar\omega$. Since low lying states (i.e., those close to the Fermi level) carry smaller values of the spin that redistribution of HFB states induces the decrease (increase) of the formation amplitude, and therefore of $\gamma_l^{(1)}$, for small (large) l values as the frequency increases, as indeed is seen in Fig. 1.

The penetration factor corresponding to the decay of ^{152}Dy, contained in the function $\gamma_l^{(2)}$, is given in Fig. 2 as a function of the α particle Q value, called Q_α in the figure. Also here the curves are labeled by l. We present $\gamma_l^{(2)}$ only for the case of ^{152}Dy because this plot gives a rather universal behavior of the penetration with the Q value, as expected.

The decay from a superdeformed band in the mother nucleus to the ground state band in the daughter nucleus can proceed through a complicated combination of electromagnetic and α decay transitions. For instance, first the mother nucleus may decay by $E2$ transitions following the superdeformed band, then a band crossing occurs and a high-energy $E1$ γ ray is emitted to another band. This process can occur
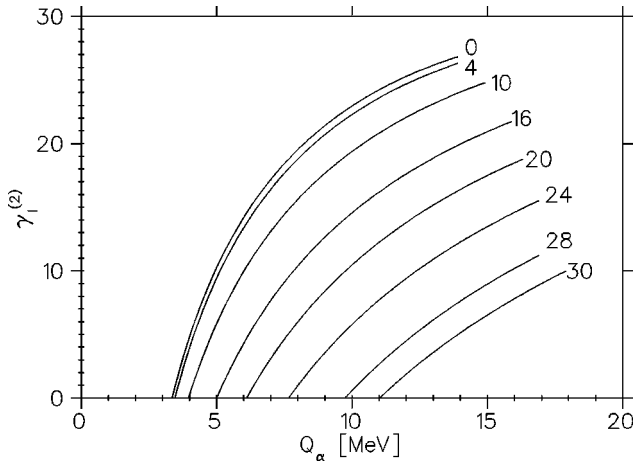
FIG. 2. The number $\gamma_l^{(2)}$ containing the penetration factor [see Eq. (3.1)] as a function of the Q value corresponding to the α decay from ^{152}Dy (Q_α). The curves are labeled by the corresponding l values.

several times to the point where a bandhead is reached. From here, finally, α decay can proceed to a band in the daughter nucleus. Even in this nucleus the decay can follow a complicated path of γ ray emissions down to the ground state. For our purpose of estimating the possibility of observing with present experimental facilities α decay from the superdeformed band it suffices to analyze two extreme cases. We assume that the mother nucleus decays by electromagnetic transitions to the head of the superdeformed band. From here α decay follows to (1) the ground state of the daughter nucleus or (2) a similar state of the daughter superdeformed band followed by an electromagnetic transition to the ground state.

We will first analyze the α decay from the superdeformed band in the mother nucleus ^{152}Dy. In this case the bandhead has an angular momentum $I_i = 24$, i.e., $\hbar\omega = 0.4$. The corresponding Q value is $Q_\alpha = 11.18$ MeV. From Fig. 1(a) one sees that for $\hbar\omega = 0.4$ one obtains the order of magnitude $\gamma_{l=24}^{(1)} \approx -18$, while for the penetration term one has, from Fig. 2, $\gamma_{l=24}^{(2)} \approx 8$. Therefore, the logarithm of the ratio between this decay and the corresponding g.s. to g.s. transition is, according to Eq. (3.1), $\gamma^{(1)} + \gamma^{(2)} \approx -10$. This small number is due to the large centrifugal barrier induced by the $l = 24$ angular momentum transfer, as seen in Figs. 1 and 2. This possibility is therefore highly unlikely.

According to possibility (2) the mother nucleus decays to a superdeformed state in the daughter nucleus with the same angular momentum. Therefore the lowest angular momentum transfer is $l = 0$ and the value of Q_α would be similar to the one corresponding to the g.s. to g.s. transition, i.e., $Q_\alpha = 3.7$ MeV. One notices that in this case the overlap integrals entering Eq. (2.15) are very close to unity (the mother and daughter nuclei have the same deformations) and therefore one should correct the term $\gamma^{(1)}$ by the order of magnitude $+6$ (overlap squared in the fifth column of the Table II, corresponding to $\hbar\omega = 0.4$). We notice from Fig. 1(a) that it is $\gamma_{l=0}^{(1)} \approx -8 + 6 = -2$ while from Fig. 2 it is $\gamma_{l=0}^{(2)} \approx -10$ (this point is actually outside the range of the figure). One then has $\gamma^{(1)} + \gamma^{(2)} \approx -12$. Therefore possibility (2) is negligible in this case.

The most favorable of the cases analyzed by us is the decay of ^{192}Pb. The spin of the head of the superdeformed band is in this case $I_i = 10$ ($\hbar\omega = 0.3$) [1]. Considering the transition of type (1), one has that the Q value is $Q_\alpha = 7.80$ MeV and from Figs. 1(b) and 2 one obtains $\gamma_{l=10}^{(1)} \approx -12$ and $\gamma_{l=10}^{(2)} \approx 15$. The logarithm of the ratio given by Eq. (3.1) is then $\gamma^{(1)} + \gamma^{(2)} \approx 3$, which is already a rather big number. But this number is still much bigger if one considers possibility (2). Assuming a transition to the state with spin $I_f = 10$ in the superdeformed band of ^{188}Hg one has $l = 0$. From Fig. 1(b) one then obtains $\gamma_{l=0}^{(1)} \approx -4 + 2 = -2$ (from Table II the correction coming from the overlap squared is $+2$) and from Fig. 2 $\gamma_{l=0}^{(2)} \approx +16$. Thus, that ratio is for this decay of the order 10^{14}, which is a very large number and, therefore, the daughter nucleus can well be reached by this process of α decay. The search and eventual measurement, of this decay would have a great importance in understanding the structure of superdeformed bands as well as the mechanisms that induce α decay.

IV. SUMMARY AND CONCLUSIONS

We have studied in this paper α decay from superdeformed nuclei. For this we have solved exactly the problem of penetration of the α particle through a deformed barrier. We have found that approximate treatments of the penetrability in terms of the deformation, such as, e.g., the WKB approximation or the classical treatment of Refs. [14], are not valid for deformations larger than $\beta_2 \approx 0.3$ (see Table I).

We have also presented a formalism to calculate the formation amplitude of α particles in superdeformed nuclei, a number which is necessary to evaluate absolute decay widths. Since this calculation requires the use of single-particle states that can describe processes occurring outside the nuclear surface, we introduced a representation consisting of the eigenvalues of two different harmonic oscillator potentials. The low lying members of the representation correspond to the standard single-particle states used to describe bound properties, while the high lying members correspond to the eigenvalues of a shallow harmonic oscillator potential. Within this representation we used the HFB approximation to describe the structure of the superdeformed nuclei. This single-particle basis allows for a much faster convergency of the computed formation amplitude in the region beyond the nuclear surface, where the interaction becomes practically a Coulomb repulsion between the emitted α particle and the daughter nucleus. We can therefore perform calculations which would otherwise be prohibitive. We have thus found that the formation amplitude (and the corresponding α decay probability) decreases with the difference between the quadrupole deformations in the mother and daughter nuclei, although this is not a big effect (see the differences between the columns labeled $\mathcal{I}_1$ and $\mathcal{I}_2$ in Table II).

We assumed that the mother nucleus decays by electromagnetic transitions to the head of a superdeformed band. From here we considered that α decay proceeds following two different possibilities: (1) direct α decay to the ground state of the daughter nucleus and (2) α decay to an excited state belonging to the superdeformed band of the daughter nucleus followed by an electromagnetic transition to the ground state. The first process involves large transferred an-

gular momenta and Q values, while for the second one those quantities are both rather small.

We found that the α decay probability from the head of a superdeformed band in ^{192}Pb to the corresponding state in ^{188}Hg is about 14 orders of magnitude larger than the corresponding probability for the ground state to ground state transition. This is therefore a likely candidate to observe α decay transitions from superdeformed bands.

ACKNOWLEDGMENTS

APPENDIX

In this appendix we give the multipole expansion of the formation amplitude, which is the generalization of the expression given in Ref. [12] to a deformed mean field. Different multipoles are used as initial conditions to integrate the system of equations (2.2), describing the motion of the α particle in a deformed Coulomb field. By considering the expansion (2.16) of the SP wave functions one obtains for the wave functions of the mother and daughter nuclei (2.14)

$$\psi_{B\pi} = \sum_{ik\,\gamma_i\gamma_k} \sum_{E,m>0} B_\pi(E,m)[c_{A\pi;E\gamma_i}^{(i)} c_{A\pi;E\gamma_k}^{(k)}$$
$$\times (-)^{j_k-m}\sqrt{2}\,\psi_{\gamma_i m}^{(\lambda_i)}(1)\psi_{\gamma_k \overline{m}}^{(\lambda_k)}(2)]\psi_{A\pi},$$

$$\psi_{B\nu} = \sum_{i'k'\,\gamma_i'\gamma_k'} \sum_{E',m'>0} B_\nu(E',m')[c_{A\nu;E'\gamma_i'}^{(i')} c_{A\nu;E'\gamma_k'}^{(k')}$$
$$\times (-)^{j_k'-m'}\sqrt{2}\,\psi_{\gamma_i' m'}^{(\lambda_i')}(3)\psi_{\gamma_k'\overline{m'}}^{(\lambda_k')}(4)]\psi_{A\nu}, \qquad \text{(A1)}$$

where B_τ, $\tau=\pi,\nu$ are the pairing densities given by Eq. (2.15). By using the standard recoupling procedure to the c.m. and relative coordinates and performing the integrals one finally obtains a multipolar expansion of the α particle formation amplitude

$$\mathcal{F}(R_\alpha,\hat{R}_\alpha') = \sum_{L_\alpha} \mathcal{F}_{L_\alpha}(R_\alpha)Y_{L_\alpha 0}(\hat{R}_\alpha')$$

$$= \sum_{iki'k'} \sum_{N_\alpha L_\alpha} W_{N_\alpha L_\alpha}^{(iki'k')}\Phi_{N_\alpha L_\alpha}^{(\Lambda_{ik}^{i'k'})}(R_\alpha,\hat{R}_\alpha'),$$
$$\text{(A2)}$$

where

$$W_{N_\alpha L_\alpha}^{(iki'k')} = \sum_{N_\pi L_\pi} \sum_{N_\nu L_\nu} G_\pi^{(ik)}(N_\pi,L_\pi)G_\nu^{(i'k')}(N_\nu,L_\nu)C_{000}^{L_\pi L_\nu L_\alpha}\sum_{n_\alpha}\langle n_\alpha 0 N_\alpha L_\alpha;L_\alpha|N_\pi L_\pi N_\nu L_\nu;L_\alpha\rangle_{D_{ik}^{i'k'}}\mathcal{I}_{n_\alpha 0}^{(\Lambda_{ik}^{i'k'}\lambda_\alpha)}, \quad \text{(A3)}$$

$$G_\pi^{(ik)}(N_\pi,L_\pi) = \sum_{\gamma_i\gamma_k} \mathcal{B}_\pi(\gamma_i,\gamma_k,L_\pi)\left\langle (l_i l_k)L_\pi\left(\frac{1}{2}\frac{1}{2}\right)0;L_\pi\right|\left(l_i\frac{1}{2}\right)j_i\left(l_k\frac{1}{2}\right)j_k;L_\pi\right\rangle\langle n_\pi 0 N_\pi L_\pi;L_\pi|n_i l_i n_k l_k;L_\pi\rangle_{D_{ik}}\mathcal{I}_{n_\pi 0}^{(\lambda_{ik}\lambda_\alpha)},$$
$$\text{(A4)}$$

$$\mathcal{B}_\pi(\gamma_i,\gamma_k,L_\pi) = \sum_{E,m>0} \frac{1+(-)^{L_\pi}}{2}B_\pi(E,m)c_{A\pi;E\gamma_i}^{(i)}$$
$$\times c_{A\pi;E\gamma_k}^{(k)}(-)^{j_2-m}\sqrt{2}C_{m\overline{m}0}^{j_i j_k L_\pi}. \qquad \text{(A5)}$$

A similar expression is obtained for neutrons. The first set of brackets in Eq. (A4) denotes $jj-LS$ recoupling coefficients while the second one is the generalized Talmi-Moshinsky symbol, which depends upon the ratio $D_{ik}=\lambda_i/\lambda_k$ [20]. The quantities $\mathcal{I}_{n_\pi 0}^{(\lambda_{ik},\lambda_\alpha)}$ are the overlap integrals between the radial HO wave functions, i.e.,

$$\mathcal{I}_{n_\pi 0}^{(\lambda_{ik},\lambda_\alpha)} = \langle R_{n_\pi 0}^{(\lambda_{ik})}|R_{00}^{(\lambda_\alpha)}\rangle, \qquad \text{(A6)}$$

with the relative HO parameter λ_{ik} given by

$$\lambda_{ik} = \frac{\lambda_i\lambda_k}{\Lambda_{ik}}, \qquad \text{(A7)}$$

where i, k refers to the basis with frequency ratios f_i, f_k [see Eq. (2.22)] and

$$\Lambda_{ik} = \frac{1}{2}(\lambda_i+\lambda_k) \qquad \text{(A8)}$$

is the c.m. HO parameter. The overlap integrals $\mathcal{I}_{n_\alpha 0}^{(\lambda_{ik}^{i'k'}\lambda_\alpha)}$ and radial c.m. wave functions $\Phi_{N_\alpha L_\alpha}^{(\Lambda_{ik}^{i'k'})}(R_\alpha\hat{R}_\alpha')$ in Eq. (A2) depend on the relative and c.m. HO parameters, respectively. That is,

$$\lambda_{ik}^{i'k'} = \frac{\Lambda_{ik}\Lambda_{i'k'}}{\Lambda_{ik}^{i'k'}}, \qquad \text{(A9)}$$

$$\Lambda_{ik}^{i'k'} = \frac{1}{2}(\Lambda_{ik}+\Lambda_{i'k'}). \qquad \text{(A10)}$$

[1] B. F. Richard and B. Singh, Report No. LBL-35916, 1994.

[2] T. R. Werner and J. Dudek, At. Data Nucl. Data Tables **50**, 179 (1992).

[3] M. L. A. de Voight, J. Dudek, and Z. Szymanski, Rev. Mod. Phys. **55**, 949 (1983).

[4] A. Faessler and R. Sheline, Phys. Rev. **148**, 1003 (1966).

[5] J. Dudek, A. Majhofer, J. Skalski, T. Werner, S. Cwiok, and W. Nazarewicz, J. Phys. G **5**, 1359 (1979).

[6] S. Cwiok, J. Dudek, W. Nazarewicz, J. Skalski, and T. Werner, Comput. Phys. Commun. **46**, 379 (1987).

[7] R. Bengtsson, J. Dudek, W. Nazarewicz, and P. Olanders, Phys. Scr. **39**, 196 (1989).

[8] H. J. Mang, Annu. Rev. Nucl. Sci. **14**, 1 (1964).

[9] J. K. Poggenburg, H. J. Mang, and J. O. Rasmussen, Phys. Rev. **181**, 1697 (1969).

[10] A. Arima and I. Tonozuka, Nucl. Phys. **A323**, 45 (1979).

[11] D. S. Delion, A. Insolia, and R. J. Liotta, Phys. Rev. C **46**, 884 (1992); **46**, 1346 (1992).

[12] D. S. Delion, A. Insolia, and R. J. Liotta, Phys. Rev. C **54**, 292 (1996).

[13] D. S. Delion, A. Insolia, and R. J. Liotta, Phys. Rev. Lett. **78**, 4549 (1997).

[14] P. O. Fröman, Mat. Fys. Skr. Dan. Vid. Selsk. **1**, No. 3 (1957).

[15] A. Raptis and A. C. Allison, Comput. Phys. Commun. **14**, 1 (1978).

[16] R. G. Lovas, R. J. Liotta, A. Insolia, K. Varga, and D. S. Delion, Phys. Rep. **294**, 265 (1998).

[17] T. L. Stewart, M. W. Kermode, D. J. Beachey, N. Rowley, I. S. Grant, and A. T. Kruppa, Nucl. Phys. **A611**, 332 (1996).

[18] P. Ring and P. Schuck, *The Nuclear Many-Body Problem* (Springer-Verlag, New York, 1980).

[19] K. Varga, R. G. Lovas, and R. J. Liotta, Nucl. Phys. **A550**, 421 (1992).

[20] M. Sotona and M. Gmitro, Comput. Phys. Commun. **3**, 53 (1972).

[21] B. Buck, A. C. Merchand, and S. M. Perez, At. Data Nucl. Data Tables **54**, 53 (1993).

[22] Y. R. Shimizu, E. Vigezzi, and R. A. Broglia, Nucl. Phys. **A509**, 80 (1990).

[23] R. Wyss (private communication).